JNeurosci
THE JOURNAL OF NEUROSCIENCE

Research Articles: Neurobiology of Disease

Zinc status alters Alzheimer's disease progression through NLRP3-dependent inflammation

https://doi.org/10.1523/JNEUROSCI.1980-20.2020

Cite as: J. Neurosci 2021; 10.1523/JNEUROSCI.1980-20.2020

Received: 29 July 2020
Revised: 27 November 2020
Accepted: 4 December 2020

Zinc status alters Alzheimer's disease progression through NLRP3-dependent inflammation.

Jack Rivers-Auty[1,2,3], Victor S Tapia[#,1,2], Claire S White[#,1,2], Michael JD Daniels[1,2], Samuel Drinkall[1,2], Paul T Kennedy[1,2], Harry G Spence[1,2], Shi Yu[1,2], Jack P Green[1,2], Christopher Hoyle[1,2], James Cook[1,2], Amy Bradley[2], Alison E. Mather[4,5], Ruth Peters[6,7], Te-Chen Tzeng[8], Margaret J Gordon[9], John H Beattie[9], David Brough[†,1,2], Catherine B. Lawrence[†,1,2].

*for the Alzheimer's Disease Neuroimaging Initiative

*Data used in preparation of this article were obtained from the Alzheimer's Disease Neuroimaging Initiative (ADNI) database (adni.loni.usc.edu). As such, the investigators within the ADNI contributed to the design and implementation of ADNI and/or provided data but did not participate in analysis or writing of this report. A complete listing of ADNI investigators can be found at: http://adni.loni.usc.edu/wp-content/uploads/how_to_apply/ADNI_Acknowledgement_List.pdf

[1]Division of Neuroscience and Experimental Psychology, School of Biological Sciences, Faculty of Biology, Medicine and Health, Manchester Academic Health Science Centre, University of Manchester, AV Hill Building, Oxford Road, Manchester, M13 9PT, U.K.

[2]Lydia Becker Institute of Immunology and Inflammation, University of Manchester, Manchester M13 9PT, UK

[3]Tasmanian School of Medicine, College of Health and Medicine, University of Tasmania, Hobart, Tasmania, Australia

[4]Quadram Institute Bioscience, Norwich Research Park, Norwich, Norfolk, NR4 7UA, UK.

[5]University of East Anglia, Norwich Research Park, Norwich, Norfolk, NR4 7TJ, UK.

[6]School of Psychology, University of New South Wales, Sydney, NSW, Australia

[7]Neuroscience Research Australia, Barker Street, Sydney, New South Wales 2031, Australia

[8]Immunology and Inflammation, Bristol-Myers Squibb (Celgene Corporation), Cambridge, MA 02140, USA

[9]Rowett Institute of Nutrition and Health, University of Aberdeen, Foresterhill, Bucksburn, Aberdeen AB25 2ZD, Scotland, UK

[#]Contributed equally to this work

[†]to whom correspondence should be addressed: Catherine B. Lawrence. Tel: +44 161 275; Email Catherine.lawerence@manchester.ac.uk: David Brough. Tel: +44 161 275 5039; Email David.brough@manchester.ac.uk.

Abbreviated title

Zinc status, inflammation and Alzheimer's disease

No figures: 5

No tables: 1

No words:

Abstract: 209

Introduction: 963

Discussion: 1142

Conflicts of interest

The authors declare no competing financial interests

Acknowledgements

Data collection and sharing for this project was funded by the Alzheimer's Disease Neuroimaging Initiative (ADNI) (National Institutes of Health Grant U01 AG024904) and DOD ADNI (Department of Defence award number W81XWH-12-2-0012). ADNI is funded by the National Institute on Aging, the National Institute of Biomedical

Imaging and Bioengineering, and through generous contributions from the following: AbbVie, Alzheimer's Association; Alzheimer's Drug Discovery Foundation; Araclon Biotech; BioClinica, Inc.; Biogen; Bristol-Myers Squibb Company; CereSpir, Inc.; Cogstate; Eisai Inc.; Elan Pharmaceuticals, Inc.; Eli Lilly and Company; EuroImmun; F. Hoffmann-La Roche Ltd and its affiliated company Genentech, Inc.; Fujirebio; GE Healthcare; IXICO Ltd.; Janssen Alzheimer Immunotherapy Research & Development, LLC.; Johnson & Johnson Pharmaceutical Research & Development LLC.; Lumosity; Lundbeck; Merck & Co., Inc.; Meso Scale Diagnostics, LLC.; NeuroRx Research; Neurotrack Technologies; Novartis Pharmaceuticals Corporation; Pfizer Inc.; Piramal Imaging; Servier; Takeda Pharmaceutical Company; and Transition Therapeutics. The Canadian Institutes of Health Research is providing funds to support ADNI clinical sites in Canada. Private sector contributions are facilitated by the Foundation for the National Institutes of Health (www.fnih.org). The grantee organization is the Northern California Institute for Research and Education, and the study is coordinated by the Alzheimer's Therapeutic Research Institute at the University of Southern California. ADNI data are disseminated by the Laboratory for Neuro Imaging at the University of Southern California. AEM is a Food Standards Agency Fellow and is supported by the Biotechnology and Biological Sciences Research Council (BBSRC) Institute Strategic Programme Microbes in the Food Chain BB/R012504/1 and its constituent projects BBS/E/F/000PR10348 (Theme 1, Epidemiology and Evolution of Pathogens in the Food Chain) and BBS/E/F/000PR10351 (Theme 3, Microbial Communities in the Food Chain). JRA was a Future Leader Fellow supported by the BBSRC fellowship grant titled 'Understanding how dietary zinc and inflammation impact healthy ageing in the brain' (BB/P01061X/1). This work was also funded by an Alzheimer Society project grant (AS-PG-2013-007) awarded to CBL and DB that funded JRA's salary. This work was also made possible through use of the University of Manchester Biological Services Facility and their expert animal husbandry, the Bioimaging Facility and the Histology Facility, whom we thank. The Histology Facility equipment that was used in this study was purchased by the University of Manchester Strategic Fund.

Abstract

Alzheimer's disease is a devastating neurodegenerative disease with a dramatically increasing prevalence and no disease-modifying treatment. Inflammatory lifestyle factors increase the risk of developing Alzheimer's disease. Zinc deficiency is the most prevalent malnutrition in the world and may be a risk factor for Alzheimer's disease potentially through enhanced inflammation, although evidence for this is limited. Here we provide epidemiological evidence suggesting that zinc supplementation was associated with reduced risk and slower cognitive decline, in people with Alzheimer's disease and mild cognitive impairment. Using the APP/PS1 mouse model of Alzheimer's disease fed a control (35mg/kg zinc) or diet deficient in zinc (3mg/kg zinc), we determined that zinc deficiency accelerated Alzheimer's-like memory deficits without modifying amyloid beta (β) plaque burden in the brains of male mice. The NLRP3-inflammasome complex is one of the most important regulators of inflammation and we show here that zinc deficiency in immune cells, including microglia, potentiated NLRP3 responses to inflammatory stimuli *in vitro* including amyloid oligomers, while zinc supplementation inhibited NLRP3 activation. APP/PS1 mice deficient in NLRP3 were protected against the accelerated cognitive decline with zinc deficiency. Collectively, this research suggests that zinc status is linked to inflammatory reactivity and may be modified in people to reduce the risk and slow the progression of Alzheimer's disease.

Significance Statement

Alzheimer's disease is a common condition mostly affecting the elderly. Zinc deficiency is also a global problem, especially in the elderly and also in people with Alzheimer's disease. Zinc deficiency contributes to many clinical disorders including immune dysfunction. Inflammation is known to contribute to the risk and progression

of Alzheimer's disease, thus, we hypothesised that zinc status would affect Alzheimer's disease progression. Here we show that zinc supplementation reduced the prevalence and symptomatic decline in people with Alzheimer's disease. In an animal model of Alzheimer's disease, zinc deficiency worsened cognitive decline due to an enhancement in NLRP3-driven inflammation. Overall, our data suggest that zinc status affects Alzheimer's disease progression, and that zinc supplementation could slow the rate of cognitive decline.

Introduction

The global prevalence of dementia (of which the most common type is Alzheimer's disease), is growing with 152 million people predicted to be living with dementia by 2050 (from 50 million in 2018), and there are no effective treatments (Alzheimers, 2015). Around 92% of people living with dementia also suffer from one or more long-term diseases (co-morbidities) (Browne et al., 2017). It has been established that disease-associated inflammation increases the risk of developing dementia, and includes inflammation associated with several co-morbidities for Alzheimer's disease such as infection, diabetes, atherosclerosis and obesity (Whitmer et al., 2005; Profenno et al., 2010). Zinc is an essential trace element obtained from the diet that regulates the expression and activation of many biological molecules. Maintenance of adequate zinc levels through a balanced diet is therefore important to health. Zinc deficiency affects up to two billion people world-wide and has profound effects on immune system function (Prasad, 2012). Given its prevalence, therefore, it is likely that zinc deficiency represents a significant co-morbidity for Alzheimer's disease that could contribute to poorer quality of life and disease outcome. Previous associations between zinc deficiency and Alzheimer's disease include several studies reporting reduced plasma zinc levels in people with Alzheimer's disease (Ventriglia et al., 2015). Overall, these data suggest that people with Alzheimer's disease are at risk of zinc deficiency, though the potential effect zinc deficiency is having on the condition is currently debated.

Zinc is a critical micronutrient that plays an essential role in a vast number of physiological processes. Approximately 10% of proteins have zinc binding domains, zinc also plays a role in membrane stabilization and can act directly as a signalling molecule (Sensi et al., 2009; Kambe et al., 2015). Because of its physiological

154 importance, its cytosolic and extracellular concentrations are tightly controlled by
155 several mechanisms including two main families of transporters, the zinc
156 transporters (ZnT) and the Zrt-Irt-related proteins (ZIP), as well as zinc storage
157 proteins (e.g. metallothioneins) and vesical storage of free zinc (Sensi et al., 2009;
158 Kambe et al., 2015). Typically, ZIP transporters act to increase cytosolic
159 concentrations of zinc, while ZnT act to decrease cytosolic concentrations by
160 movement of zinc out of the cell or into cellular compartments including vesicles,
161 Golgi and endosomes (Sensi et al., 2009; Kambe et al., 2015). The ubiquity and
162 diversity of molecular functions which involve zinc has made researching the
163 interactions between zinc status and Alzheimer's disease difficult.
164
165 Several potential pathophysiological links of Alzheimer's disease and zinc status
166 have been investigated. The role zinc binding has in amyloid fibril formation has
167 been a substantial area of interest. Several *in vitro* and *in vivo* studies report that
168 excessive zinc promotes the formation of amyloid oligomers and fibrils through direct
169 zinc-amyloid interactions. Amyloid oligomers and fibrils are one of the pathological
170 hallmarks of Alzheimer's disease and considered a likely driver of the disease (Esler
171 et al., 1996; Brown et al., 1997; Lee et al., 2018). These findings have driven
172 preliminary Alzheimer's clinical trials on compounds, such as PBT2, which increase
173 cellular uptake of zinc thereby reducing extracellular zinc levels. These trials have
174 had largely positive results (Faux et al., 2010).
175
176 Another focus of the Alzheimer's disease zinc field is the role of zinc proteases in
177 beneficial and pathological processes. Zinc is an essential co-factor in a range of
178 proteases including proteases that cleave the amyloid precursor protein into non-
179 pathogenic peptides including the a-disintegrin and metalloproteinases (ADAMs)

(Gough et al., 2011). Zinc is also a co-factor in proteases that digest the pathological forms of amyloid into non-oligomerising products, including the insulin degrading enzyme (Gough et al., 2011). Finally, the zinc protease matrix metallopeptidase 9 (MMP9) plays a critical role in the healthy functioning of central nervous system, particularly the activation of brain derived neurotrophic factor (BDNF) (Yang et al., 2014; Frazzini et al., 2018). BDNF is an important neurotrophin that plays a role in neuronal plasticity and synapse formation. Previously, the administration of zinc chelators in mice has been shown to lower active BDNF levels impairing cognitive performance (Yang et al., 2014; Frazzini et al., 2018). While zinc and Alzheimer's disease has been an active field of research, little attention has been given to the known effects of zinc status on immune function; particularly neuroinflammation, an established driver of Alzheimer's disease pathology.

We previously reported that zinc depletion of macrophages activates an inflammatory complex called the NLRP3 (NACHT, LRR and PYD domains-containing protein 3) inflammasome driving release of the pro-inflammatory cytokine interleukin-1β (IL-1β) from the cell (Summersgill et al., 2014). The NLRP3 inflammasome is formed in macrophages, and microglia in the brain, in response to pathogenic or damage associated stress and drives an inflammatory response. The NLRP3 inflammasome complex is composed of NLRP3, the adaptor protein ASC (apoptosis-associated speck-like protein containing a caspase activation and recruitment domain (CARD)), and the protease caspase-1 which is responsible for cleaving the inactive precursor pro-IL-1β to an active secreted IL-1β molecule (Brough et al., 2017; Heneka et al., 2018). The NLRP3 inflammasome is suggested to contribute to the damaging inflammation that worsens Alzheimer's disease (Heneka et al., 2013; Daniels et al., 2016; Dempsey et al., 2017; White et al., 2017;

Heneka et al., 2018). NLRP3 is also suggested to contribute to age-related cognitive decline (Youm et al., 2013).

This study aimed to test the hypothesis that zinc status can influence the development of Alzheimer's disease. We report here that zinc supplementation in people reduced the prevalence and symptomatic decline of Alzheimer's disease, and that zinc deficiency in an Alzheimer's disease mouse model accelerated cognitive decline through potentiation of NLRP3-dependent inflammation, an effect which was reversible. These data suggest that zinc deficiency is a treatable co-morbidity, which if managed correctly, potentially through the use of zinc supplementation, could slow the rate of cognitive decline in people with Alzheimer's disease.

Materials and Methods

Epidemiological study

Data acquisition

Data used in the preparation of this article were obtained from the Alzheimer's Disease Neuroimaging Initiative (ADNI) database (adni.loni.usc.edu). The ADNI was launched in 2003 as a public-private partnership, led by Principal Investigator Michael W. Weiner, MD. The primary goal of ADNI has been to test whether serial magnetic resonance imaging (MRI), positron emission tomography (PET), other biological markers, and clinical and neuropsychological assessment can be combined to measure the progression of mild cognitive impairment (MCI) and early Alzheimer's disease. The subjects were recruited from over 50 sites across the U.S.A and Canada. ADNI has undergone three stages of recruitment each with differences in the imaging and biomarker analyses, these have been named ADNI-1, ADNI-GO and ADNI-2. Collectively these protocols have recruited 1631 adults into

the study consisting of age appropriate cognitively normal individuals, people with early or late MCI, and people with early Alzheimer's disease. The follow up duration of each group is specified in the protocols for ADNI-1, ADNI-2 and ADNI-GO with 120 months as the maximum. Subjects were evaluated upon entry into the study, then at the 6 and 12 month time points, and yearly after this. For up-to-date information, see www.adni-info.org.

Epidemiological analyses

Epidemiological analyses were performed as described in Rivers-Auty *et al.(2020)*. Briefly, datasets containing the medical history (RECMHIST.csv), recurrent medicines (RECCMEDS.csv) and patient summary data (ADNIMERGE.csv) were downloaded on the 3rd of May 2018. String search methods were applied to identify patients using supplements. Baseline statistics were extracted, and logistic regression was performed on Alzheimer's disease prevalence to evaluate the association between supplement use and Alzheimer's disease risk. Negative binomial generalised linear mixed modelling (GLMM) was applied to the number of failures which occurred during the mini-mental state examination (MMSE). Variables were included in the models both as a fixed effect and as an interaction effect with time. Variables included in the analyses were diagnosis (control, MCI or Alzheimer's disease), age, gender, APOE4 genotype, education level, headaches, arthritis, diabetes, smoking, cardiovascular risk factors, and supplement use. The significance of variable inclusion for the logistic regression and GLMM was evaluated using the log likelihood ratio test, estimated by a Chi-squared distribution. To construct the negative binomial GLMM models the package glmmadmb was used (Fournier et al., 2012; Skaug et al., 2013), logistic regression utilized the LME4 package (Bates et

al., 2015), both on R version 3.5.1 (R Core Team 2018) with RStudio version 1.1.453 (RStudio Team 2016). Details of the full analysis can be found in the Extended Data.

Animal experiments

Animals were housed in individually ventilated cages maintained at 21 (± 2) ^{0}C with 40-50% humidity on a standard 12h light/dark cycle and free access to water and food. Prior to experiment all animals were on standard rodent chow (BK001 E, Special Diets Services, UK). Genotyping was performed by Transnetyx™ and these results were not revealed until the end of all behavioural, histological or physiological investigations had been completed. Thus, all experiments were performed blinded to genotype. All behavioural videos, physiological analyses and histological quantifications were recoded to blind the experimenter to both genotype and diet. Diet was randomly allocated by cage using the TrueRandom™ software. All behavioural experiments were performed with 40db white noise played in surround sound to avoid auditory cues. All animal experiments were carried out in accordance with the United Kingdom Animals (Scientific Procedures) Act 1986 and approved by the Home Office and the local Animal Ethical Review Group, University of Manchester.

The effect of zinc deficiency in APP/PS1 mice

APPswe PSEN1ΔE9 (APP/PS1) transgenic mice on a C57BL/6J background were obtained from the Jackson Laboratory™ (#005864). Hemizygous male APP/PS1 mice were bred with C57BL/6J female mice to generate litters of hemizygous APP/PS1 and C57BL/6J (wild-type; WT) littermate controls, of which the males were used in the experiments. At three months of age the animals underwent baseline behavioural testing and were then randomly allocated to a zinc normal (ZN) diet (35

mg/kg, Table 1) or zinc deficient (ZD) diet (3 mg/kg, Table 1). Two thirds of the mice were initially placed on a ZD diet and one third was placed on a ZN diet. After three months on diet another set of behavioural tests were performed. Then half the cages on a ZD diet were randomly allocated to be placed on the ZN diet. All mice remained on diet for another three months, which was followed by another set of behavioural experiments after which mice were sacrificed by exsanguination and cardiac perfusion with saline under isoflurane (2-5%) anaesthesia. A power analysis was performed using the standardized effect size based on an ordinary least squared repeated measures method. A moderate partial η^2 of 0.15 was selected with an α of 0.05 and a β of 0.2. From this it was found an *n* of 10 was required. To account for attrition and fluctuations in genotype prevalence a target of *n* = 13 was selected. Final numbers (*n*) in each group were as follows: WT ZN = 13; WT ZD = 15; WT ZD/ZN = 12; APP/PS1 ZN = 13; APP/PS1 ZD = 11; APP/PS1 ZD/ZN = 11.

The effect of zinc deficiency in aged C57BL/6J mice

At three months (Young) or 20 months (Aged) of age C57BL/6J mice had their baseline memory performance probed utilizing the Y-maze task, before being randomly allocated to a ZD or ZN diet for three months (*n* = 15 per group). All mice were then evaluated in the Y-maze and culled by exsanguination and cardiac perfusion with saline under isoflurane (2-5%) anaesthesia. Using the same power analysis as above an *n* of 15 was selected to account for the greater potential of attrition.

The effect of zinc deficiency in APP/PS1 mice deficient in NLRP3

Mice lacking NLRP3 ($NLRP3^{-/-}$) on a C57BL/6J background mice were provided by Dr. Vishva Dixit (Genentech) (Mariathasan et al., 2006). These mice were

backcrossed with the APP/PS1 line for 6 generations and then bred into two colonies containing APP/PS1/NLRP3$^{-/-}$ hemizygous male and WT/NLRP3$^{-/-}$ (WT are C57BL/6J) female breeders, and APP/PS1/NLRP3$^{+/+}$ hemizygous male and WT/NLRP3$^{+/+}$ female breeders. These were used to generate the experimental male mice used in this study. At three months of age, cages of mice were randomly allocated onto either a ZD or ZN diet. After six months on diet, memory of all mice was assessed with the Y-maze task. The animals were then sacrificed by exsanguination and cardiac perfusion with saline under isoflurane (2-5%) anaesthesia. The primary outcome of Y-maze performance after 6 months on diet was selected. Using the data obtained in the zinc deficiency experiment above, the mean difference of 13.4 and a pooled standard deviation of 7.6 was used with an α of 0.05 and a β of 0.2. This analysis found an *n* of 9 mice per group was required for the Sidak corrected post-hoc analysis with 6 comparisons. To account for attrition and fluctuations in genotype prevalence a target *n* = 10 was selected. Final numbers (*n*) in each group were as follows: WT/NLRP3$^{+/+}$ ZN = 12; WT/NLRP3$^{+/+}$ ZD = 14; WT/NLRP3$^{-/-}$ ZN = 8; WT/NLRP3$^{-/-}$ ZD = 9; APP/PS1/NLRP3$^{+/+}$ ZN = 8; APP/PS1/NLRP3$^{+/+}$ ZD = 11; APP/PS1/NLRP3$^{-/-}$ ZN = 13; APP/PS1/NLRP3$^{-/-}$ ZD = 9.

Y-maze task

The Y-maze consisted of three connected small rooms each with a unique visual cue on the back wall. Mice were placed in the maze using the tube transfer method and allowed to explore for 8 min. The exploration was recorded, and the videos were then recoded and scored by an observer blinded to the experimental groups. A successful set of alternations was defined as entering all three rooms in succession with no repeated room entries. Performance was expressed as the percentage of

total alternation sets which were successful. The mazes were thoroughly cleaned with 70% ethanol and then dried with paper towels between animals to avoid olfactory cues. Trials in which the mouse completed less than 9 entries were excluded.

Novel smell task

The novel smell task was performed in a cylindrical arena. The mice were first habituated to the arena without olfactory cues by being placed in the arena using the tube transfer method for 8 min. The following day the mice were placed in the arena for 8 min with two olfactory cue dispensers with identical smells. They were then placed in holding cages for 8 min, while the arenas were cleaned with ethanol and dried, and the olfactory dispensers where changed to consist of a novel and familiar smell. The mice were then placed back in the area and recorded for 4 min. The exploration was recorded, the videos were then recoded and timed using the Novel Object Timer program (https://jackauty.com/program/) by an observer blinded to the experimental groups as described in Daniels et al. (Daniels et al., 2016). Trials in which the mouse completed less than 4 sec of exploration were excluded.

Tissue processing

Mice were terminally anaesthetised with 2-5% isoflurane (30% O_2, 70% N_2O). Plasma was collected via cardiac puncture using citrate-treated needles, followed by trans-cardiac perfusion with 0.9% saline. Femurs were taken for ICP-Mass spectrometry of the bone and one epididymal fat pad was removed and weighed. Brains were dissected into hemispheres. The left hippocampus was extracted and

snap frozen for RNA-sequencing. RNA was extracted using a Qiagen mini-kit as per instructions and tested for purity and concentration using the nano-drop method and analysed for purity and digestion with a TAPE station. All samples had RNA integrity numbers (RIN) of over 8.5. RNAseq was performed as described in Hoyle et al. (2018) on an Illumina HiSeq4000 instrument. The right hemisphere was immerse-fixed in 4% paraformaldehyde for 24 h and cryoprotected in 30% sucrose before being snap frozen and sectioned (15 µm) coronally every 90 µm from the rostral end of the cortex (for experiment in Figs 2 and 3*A*-*C*), or immerse-fixed in 4% paraformaldehyde for 24 h then dehydrated, paraffin embedded, and sectioned (5 µm) every 100 µm from the central sulcus (for experiment in Fig 5) and mounted onto Superfrost™ Plus slides (VWR). Six sections evenly spaced throughout the cortex were selected for immunohistochemistry. Paraffin sections were deparaffinised with xylene emersion and rehydrated in descending concentrations of ethanol. For all sections, antigen retrieval consisted of 30 min immersion in 0.2 mM citrate buffer pH 6 at 96^0C followed by 10 min in 90% formic acid. Sections were washed (3x 5 min) with 0.1% tween in phosphate buffered saline (PBST), blocked for 1 h in a 1% bovine serum albumin (BSA, A9647 Sigma-Aldrich), 0.2 M phosphate buffer (PB) solution and then incubated overnight in 1:200 biotinylated 6e10 antibody (for amyloid beta (Aβ) plaques; #SIG-39340-200, Covance) or 1:1000 Iba1, (for microglia; Wako Ltd) in a 1% BSA, 0.2 M PB solution at 4^0C. Sections were then washed (3x 5 min, PBST), incubated with biotinylated anti-mouse secondary (Iba1), or/followed by, 1:20 Strep-Avidin (P188503, RnD)/1% BSA, 0.2 M PB solution for 2 h at room temperature, washed and then visualised with a DAB-nickel solution (D0426-50SET, Sigma-Aldrich). Sections were dehydrated in serial ethanol solutions of increasing concentration and then 100% xylene, and then mounted with DPX (DI5319/05, Fisher Scientific). The slides were scanned, and the images recoded. Aβ

plaque burden, approximated as percentage stained area, was calculated utilizing threshold-particle analyses performed on ImageJ. The microglial activation stage was performed as in Daniels et al. (Daniels et al., 2016).

Laser microdissection

Eight to nine-month-old APP/PS1 and C57B/6J littermate mice were terminally anaesthetised with 2-5% isoflurane (30% O_2, 70% N_2O) followed by trans-cardiac perfusion with 0.9% saline. Brains were harvested, snap frozen using dry ice and stored at -80 °C until analysed. Coronal 30 µm brain sections were taken from the hippocampal region utilising Leica CM3050 S cryostat and mounted onto RNase-free membrane-coated microscopy slides (Molecular Machines & Industries). The slides were stained by immersion in a filtered Congo red solution (0.2% Congo red solution in 20% NaCl, 80% ethanol, pH 9.0) for 20 min at room temperature. Using the laser microdissection (LMD) MMI (Molecular Machines & Industries) SmartCut software, UV laser excised discs of a fixed 100 µm diameter with Congo Red stained amyloid-plaques in the centre were cut (Fig. 3*H*). Plaque-free tissue from both the same animals and WT littermate controls were also cut and collected separately. Once cut, microdissected regions were acquired using mechanically operated adhesive MMI Isolation Caps (Molecular Machines & Industries), which were subsequently filled with the lysis buffer component of RNeasy Micro Kit (Qiagen). On completion of LMD, sample-containing microcentrifuge tubes immediately underwent lysis via freeze-thaw cycling and brief (< 5 sec) sonication. Purified RNA was acquired as per RNeasy Micro Kit (Qiagen) instructions with on-column DNase digestion and washing according to manufacturer's guidelines. Images were collected on an Olympus IX83 inverted microscope modified for LMD capture.

ICP-Mass spectrometry

Inductively coupled plasma mass spectrometry (ICP-MS) (Agilent 7900) was used to assess zinc levels in the plasma and bone. The diets, bedding, drinking water and cage materials were also measured for zinc content prior to the start of the experiments. As a result of these analyses, the bedding was changed to the low zinc nesting material Wood Wool (TAPVEI®). Plasma samples were diluted in 1:10 with 0.1 M hydrochloric acid, centrifuged (2500 g) and then analysed with appropriate standards generated. Whole femurs were taken from the mice and wet-ashed by HNO_3 (0.5 ml, concentrated) immersion at room temperature for 24 h, then dried at 60 °C. After cooling, 0.2 ml of H_2O_2 was added and the samples were incubated for 1 h in a drying oven at 60 °C. The solutions were diluted to 10 ml using deionised water and analysed.

Quantitative Reverse Transcription PCR

Isolated RNA was reverse-transcribed using Tetro cDNA Synthesis Kit (Bioline), with samples being incubated at 25 °C for 10 min, 45 °C for 30 min and 85 °C for 5 min. cDNA was subjected to qPCR using the 7900HT Fast Real-Time PCR detection system (Applied Biosystems) Power SYBR® Green Master Mix (Applied Biosystems). A standard amplification programme (1 x 2 min cycle at 50 °C, 1 x 10 min cycle at 95 °C, 50 x 15 sec cycle at 95 °C and 1 x 1 min cycle at 60 °C) was used for all amplifications. Primers used for the amplification were as follows: TREM2 (forward; TGGGGACCTCTCCACCAGTT, reverse; GTGGTGTTGAGGGCTTGG), NLRP3 (forward; GCCCAAGGAGGAAGAAGAAG, reverse; TCCGGTTGGTGCTTAGACTT), and IL-1β (forward; AACCTGCTGGTGTGTGACGTTC, reverse; CAGCACGAGGCTTTTTTGTTGT). Standard curves of serial control cDNA dilutions were used to determine the fold

differences in target cDNA expression. HMBS was used as the housekeeping gene (forward; GAAATCATTGCTATGTCCACCA, reverse; GCGTTTTCTAGCTCCTTGGTAA).

Cell isolation and culture

BMDM

All primary cells were harvested from 8-16-week-old, mixed sex, C57/BL6J mice (Charles River, UK) which were euthanised with rising CO_2 concentration. Murine bone-marrow derived macrophages (BMDMs) were generated as reported previously in Daniels *et al.* (Daniels et al., 2016). Briefly, BMDMs were collected by flushing bone marrow from femurs and cultured in Dulbecco's Modified Eagle's Medium (DMEM) (Gibco) supplemented with 10% foetal bovine serum (FBS) (Biowest), 1% PenStrep, 2 mM, 1% L-glutamine (Sigma) and 20% M-CSF (macrophage colony-stimulating factor)-conditioned medium from L929 cells. Cells were grown for 7 days and then scraped, counted and seeded for 24 h in 24 to 96 well plates at 1 x 10^6 cells/ml in complete DMEM. After media change, cells were primed with bacterial endotoxin (lipopolysaccharide (LPS), 1 µg/ml) from *Escherichia coli* O26:B6, for 4 h. The media was changed to serum free DMEM prior to treatment with pathway inhibitors (MCC950 10 µM or $ZnCl_2$) or vehicle (DMSO) for 15 min followed by stimuli treatment for 4 h with TPEN (N,N,N′,N′-tetrakis(2-pyridinylmethyl)-1,2-ethanediamine), or silica (<15 µm, MIN-U-SIL 15; 300 µg/ml), or 24 h for amyloid 1-42 (Sigma, oligomerised at 37^0C for 24 h in PBS prior to treatment. N.B for amyloid, cells without LPS-priming were used). Supernatants were taken for enzyme-linked immunosorbent assay (IL-1β) (ELISA) and western blot. An in-well lysis was performed with 1% Triton for western blot analyses of cytosolic and secreted proteins.

Mixed glia

Murine mixed glia cells were prepared from the brains of 2–4-day-old C57BL/6J mixed sex mice. Briefly, the cerebral hemispheres were dissected, and the meninges were then removed. The remaining tissue was homogenized in DMEM containing 10% FBS and PenStrep *via* repeated trituration. The resulting homogenate was centrifuged at 500 x *g* for 10 min, and the pellet was resuspended in fresh culture medium, seeded directly into 24-well plates and incubated at 37 °C, 90% humidity, and 5% CO_2. After 5 days, the cells were washed, and fresh medium was placed on the cells. The medium was then replaced every 2 days. Cells were used after two weeks. Cells were primed with LPS (1 µg/ml, 3 h) in DMEM containing 10% FBS and PenStrep. For zinc chelation experiments, cells were washed once with serum-free DMEM prior to treatment with serum-free DMEM containing vehicle (DMSO) or TPEN (20 µM, 4 h) with or without silica (300 µg/ml) or MCC950 (10 µM). For the amyloid experiment LPS-primed cells were made zinc deficient (TPEN, 10 µM) and incubated in amyloid oligomers (10 µg/ml, 4 h). The supernatant was centrifuged at 12,000 x g for 10 min prior to analysis for IL-1β content by ELISA.

ELISA and Western blot

IL-1β release was quantified by ELISA (DuoSet, R&D Systems) according to the manufacturer's instructions. IL-1β, gasdermin D and caspase-1 cleavage was determined by western blot. All supernatants or in-well lysates were separated by 12 well, 1.5 mm Tris-glycine SDS/PAGE and then transferred onto nitrocellulose or PVDF membranes at 25 V using a semidry Trans-Blot Turbo system (Bio-Rad). Membrane blocking was performed using in 2% bovine serum albumin (BSA) in 1% (vol/vol) Tween 20/PBS (PBST). Membranes were then incubated with primary

antibodies at 4 °C overnight (IL-1β AF-401,R&D; gasdermin D ab209845, Abcam; and caspase-1 EPR16883, abcam), washed and then labelled with HRP-conjugated secondary antibodies (2 h at room temperature). Target proteins were then visualized with Amersham ECL detection reagent (GE Healthcare) using the G:Box Chemi XX6 (Syngene) system.

ASC Oligomerization Assay.

Cells were lysed in-well with 1% Triton X-100 and protease inhibitor cocktail. Cell lysates were centrifuged at 6,800 x g for 20 min at 4 °C to separate the Triton X-100 soluble and insoluble fraction. The Triton X-100 insoluble fraction was chemically crosslinked with 2 mM disuccinimidyl suberate (DSS) (Thermo Fisher) for 30 min at room temperature. Crosslinked pellets were precipitated by centrifugation at 6,800 x g for 20 min and resuspended in Laemmli buffer. Oligomerised ASC were then detected by western blot.

ASC Speck Formation.

Adult microglia were extracted from 8-16-week-old, mixed sex, C57/BL6J mice expressing ASC-citrine on a CAG promoter using MACS® MicroBeads on digested brains as per manufacturer's instructions. Microglia were seeded for 2 h into 96-well plates at 0.5 x 10^5/ml. They were primed with LPS (1 µg/ml, 2 h). All cells were treated with the pan-caspase inhibitor Z-VAD-FMK (50 µM) prior to simulation to prevent caspase dependent cell death. Without media change, NBC19 (10 µM), MCC950 (10 µM) or vehicle (DMSO) were spiked into the appropriate wells, followed by TPEN administration (final concentration 10 µM). At 15-min intervals images were captured using a 20×/0.61 S Plan Fluor objective for a total of 12 h. Speck formation

was quantified using an IncuCyte ZOOM System (Essen Bioscience). All experiments performed in serum free OptiMEM.

Experimental statistics

All data are presented as mean values ± standard error of the mean (SEM) unless stated. For repeated measures analyses, linear mixed modelling was used to evaluate the significance of the effect of independent factors (genotype, diet and time) on the dependent variable. All factors and interactions were modelled as fixed effects and mouse identifier as a random variable. A within-subject design with random intercepts was used for all models. The significance of inclusion of an independent variable or interaction terms was evaluated using log-likelihood ratio (Bates et al., 2015). Holm-Sidak post hocs were then performed for planned pair-wise comparisons using approximated least square means (Lenth, 2016). For the remaining data, statistical analyses were unpaired Welch corrected Student's *t* test, or one-way, two-way or three-way analysis of variance (ANOVA) test depending on the number of experimental groups and independent variables in the analyses. Holm-Sidak post hocs were then performed for planned pair-wise comparisons. Homoscedasticity and normality were evaluated graphically using predicted verses (Pearson) residuals and Q-Q plots, respectively, and transformations and/or corrections were applied where necessary. All analyses were performed using R (version 3.3.3) (R Core Team; RStudio Team.). Accepted levels of significance were $^{*}p < 0.05$, $^{**}p < 0.01$, and $^{***}p < 0.001$.

Results

Zinc supplementation use is associated with reduced prevalence of Alzheimer's disease and slower cognitive decline during disease development.

The ADNI dataset was used to investigate the effects of mineral supplementation on both the prevalence of cognitive dysfunction including early and late MCI, and Alzheimer's disease, as well as the progression of cognitive decline over time. Investigating the six most common mineral supplements (calcium, iron, magnesium, multi-vitamin, selenium, zinc), and utilizing logistic regression adjusting for common confounding variables, we found that calcium, iron, magnesium and zinc supplement use was associated with significantly reduced Alzheimer's disease prevalence compared to those not taking any supplements (Fig. 1*A,B*). To further investigate the potential effects of mineral supplementation, innovative statistical methods for analysing cognitive decline, as measured by the MMSE, were employed. From this it was found that zinc supplementation was associated with significantly less cognitive decline (Fig. 1*C,E*). Other supplements, including the divalent cations calcium and magnesium, were not associated with significant changes in cognitive decline (Fig. 1*D*).

Subclinical zinc deficiency accelerates memory deficits in an animal model of Alzheimer's disease without effecting plasma zinc or weight gain

We then sought to establish that the association between zinc supplementation and improved Alzheimer's disease outcome was causal by using the APP/PS1 mouse model of Alzheimer's disease. WT control, or APP/PS1 mice were fed a diet containing the recommended zinc intake levels for mice (35mg/kg, zinc normal, ZN) or a diet that would induce a mild subclinical zinc deficiency (3mg/kg, zinc deficient, ZD) (Fig. 2*A*). Animals were put on diet from three months of age and maintained for six months with memory tests (Y-maze and novel smell test) performed at three-month intervals (Fig. 2*A*). To determine if any effects of zinc deficiency were reversible, one group of mice was maintained on a zinc deficient diet for three

months and then placed on a normal zinc diet for three months (Fig. 2*A*). APP/PS1 mice do not show altered cognitive behaviour in short term memory tasks such as the Y-maze, T-maze or novel object recognition before nine months of age (Webster et al., 2014). At the end of the experimental period animals were sacrificed zinc levels measured in the plasma and bone, and a number of histological and physiological measures taken including RNAseq on hippocampal tissue, and analyses on Aβ plaque burden and microglia morphology. There was no change in plasma zinc between all groups (diet main effect: $F(2,68)=0.86$, $p=0.43$) but a decrease in zinc content in the bone was seen in WT and APP/PS1 mice fed a zinc deficient diet indicating a change in long-term zinc status (Fig. 2*B,C*), (diet main effect: $F(2,64)=4.26$, $p=0.018$). Severe zinc deficiency can lead to weight loss, but the marginal zinc deficient diet used here had no effect on body weight compared to normal diet (Fig. 2*D*), (diet main effect: $F(2,43)=0.49$, $p=0.616$) or fat mass (data not shown, diet main effect: $F(2,74)=0.14$, $p=0.866$) of the WT or APP/PS1 mice. These data suggest that we had modelled a sub-clinical level of zinc deficiency (Beattie et al., 2012).

The mild zinc deficiency cause reversible cognitive decline in the APP/PS1 mice while having no effect on the cognitive performance of the WT mice (Y-maze task 3-way interaction: $\chi^2(6)=19.33$, $p=0.004$). In WT mice there was no effect of zinc deficient diet on memory over 6 months as analysed by the Y-maze ($Z=-0.16$, $p=1.000$) and novel smell tests ($Z=-0.16$, $p=0.743$), (Fig. 2*E,G*). As expected, the APP/PS1 mice showed no significant reduction in cognitive performance over the course of the experiment on the zinc normal diet in the Y-maze ($Z=-1.81$, $p=0.281$) or novel smell tests ($Z=-0.05$, $p=1.000$), (Fig. 2*F,H*). However, APP/PS1 mice on a zinc deficient diet showed accelerated memory loss at three months in the Y-maze test

(Z=-2.81, p=0.024), and this was worse after six months on the zinc deficient diet (Z=-3.75, p=0.001), (Fig. 2*F*). This cognitive impairment measured by Y-maze of APP/PS1 mice fed a zinc deficient diet for three months was reversed by returning the mice to a zinc normal diet for three months (Z=-3.93, p<0.001), (Fig. 2*F*). Similar, but less dramatic, trends were observed in the novel smell test in response to a zinc deficient diet in the APP/PS1 mice (Fig. 2*H*), (3-way interaction: $\chi^2(6)=14.53$, p=0.024). These data suggest that zinc deficiency is causally accelerating cognitive decline in Alzheimer's disease and that these cognitive deficits are reversible. They also place our epidemiological observations in people in context, suggesting the association of improved cognitive outcome in patients taking zinc supplements is due to a direct causal relationship between zinc status and Alzheimer's disease progression.

Zinc deficiency does not alter plaque burden, microglia activation or age-related cognitive decline

The effects of zinc deficiency on memory were not because of altered Aβ plaque burden as plaque burden was not significantly different between APP/PS1 mice fed a zinc normal or a zinc deficient diet (Fig. 3*A,B*), (2-way interaction: F(3,61)=1.93, p=0.154). Similarly, levels of microglia with activated morphology, typically associated with plaques, were not altered between treatment groups (Fig. 3*C*), (2-way interaction: F(3,49)=0.06, p=0.940). We then hypothesised that the effects of zinc deficiency may be common with NLRP3-dependent age-related cognitive decline (Youm et al., 2013). Thus, we placed 20-month-old C57BL/6J mice on a zinc deficient diet for three months, with 3-month-old mice as young controls. No acceleration in cognitive decline after a zinc deficient diet was observed at either age in the Y-maze task (3-way interaction: $\chi^2(7)=7.34$, p=0.394) or Morris water maze

task (interaction term: F(1)=0.284, p=0.570), indicating the effect of zinc deficiency seen in the APP/PS1 mice was specific to amyloidopathy and its downstream effects (Fig. 3*D,E*). To elucidate the mechanism of zinc deficiency-induced cognitive decline in APP/PS1 mice, RNAseq was performed on the whole hippocampal homogenate. However, no substantial differences in transcriptome were observed between genotype or diet (Fig. 3*F,G*). We hypothesised therefore that transcriptional differences could be occurring primarily in the periplaque regions, which were masked in the hippocampal RNAseq data (Fig. 3*F,G*) by homogenising the whole tissue. To investigate this potential locality of transcriptional changes, we utilised laser capture microdissection to probe gene expression in the periplaque regions of 8-9-month-old APP/PS1 mice (Fig. 3*H*). Performing qPCR on the established the Alzheimer's disease linked gene TREM2 and the inflammatory genes for NLRP3 and IL-1β, we confirmed that transcriptional changes were largely confined to the periplaque regions (Fig. 3*I*), (periplaque main-effect: TREM2 $\chi^2(1)=28.40$, $p<0.001$; IL-1 $\chi^2(1)=32.21$, $p<0.001$; NLRP3 $\chi^2(1)=13.93$, $p<0.001$). Given that NLRP3 activation has been strongly linked to memory impairment in Alzheimer's disease (Heneka et al., 2013; Daniels et al., 2016) and that NLRP3 is activated by zinc deficiency (Summersgill et al., 2014), we hypothesised that accelerated memory impairment in the APP/PS1 mice on the zinc deficient diet is due to a periplaque NLRP3 response (Heneka et al., 2013; Daniels et al., 2016; Dempsey et al., 2017; Venegas et al., 2017; White et al., 2017).

Zinc deficiency activates the NLRP3 inflammasome and potentiates NLRP3 responses to stimuli, while zinc supplementation inhibits NLRP3 activation

To investigate the potential regulation of NLRP3 by zinc status *in vitro* methods were employed. We previously established that primary BMDMs have similar NLRP3

responses as microglia, mixed glial cultures and *ex vivo* brain tissue slices, therefore, represent a robust, and high throughput method for investigating NLRP3 activation (Daniels et al., 2016; Hoyle et al., 2020). BMDMs were primed with LPS and then treated with the zinc chelator TPEN (1-30 μM, 4 h) to cause zinc depletion. Analysis of the supernatant showed TPEN-induced zinc depletion induced-1β release in a concentration dependent manner ($F(4,20)=25.28$, $p<0.001$), (Fig. 4*A*). Zinc depletion (TPEN 10 μM, 4 h) in LPS-primed BMDMs also caused oligomerisation of ASC, caspase-1 activation, and gasdermin-D cleavage, and this was NLRP3 dependent as it was inhibited by the selective NLRP3 inhibitor MCC950 (Fig. 4*Bi*). Conversely, zinc supplementation (with $ZnCl_2$) in LPS-primed BMDMs blocked established NLRP3 activators, including silica, by inhibiting IL-1β release ($F(5,12)=122.0$, $p<0.001$), ASC oligomerisation, caspase-1 and gasdermin D cleavage (Fig. 4*Bii,C*). We then investigated potential interactions between Aβ and zinc depletion. Utilizing BMDMs we found that only Aβ42 oligomer treatment followed by TPEN was sufficient to induce IL-1β secretion, which was inhibited by MCC950 (Fig. 4*D*). The effects of TPEN were then confirmed in LPS-primed mixed glial cultures, and again TPEN treatment induced IL-1β release which was inhibited by MCC950 ($F(5,12)=20.18$, $p<0.001$), (Fig. 4*E*). Using LPS-primed mixed glia we also found that TPEN was also able to exacerbate Aβ42 oligomer-induced IL-1β secretion ($F(3,8)=8.06$, $p=0.008$), (Fig. 4*F*). To investigate if TPEN-induced zinc depletion caused inflammasome specks in microglia, ASC-citrine expressing microglia were isolated from adult mice (Tzeng et al., 2016). Zinc depletion resulted in speck formation which was observed with live cell imaging and the NLRP3 inhibitors MCC950 (Coll et al., 2015) and NBC19 (Baldwin et al., 2017) were found to inhibit ASC speck formation (Fig. 4*G,H*), (MCC950 $Z=-6.34$, $p<0.001$; NBC19 $Z= -26.80$, $p<0.001$). Collectively, these experiments indicate that zinc status can influence

NLRP3 activity. Zinc deficiency acts as an NLRP3 activating and potentiating stimuli in macrophages, microglia and mixed glia, while zinc supplementation is inhibitory of NLRP3 activation. Critically, we found that the combination of zinc deficiency and amyloidopathy are sufficient to induce NLRP3 activation and IL-1β release in mixed glia (and macrophages).

Zinc deficiency accelerates cognitive decline in the APP/PS1 mouse model of Alzheimer's disease through an NLRP3 dependent mechanism

As we had established that zinc deficiency could potentiate NLRP3 responses *in vitro* we hypothesised that zinc deficiency accelerated cognitive impairment in the APP/PS1 mouse via the NLRP3 inflammasome. To test this hypothesis, we crossed WT and APP/PS1 mice with NLRP3$^{-/-}$ mice to generate four experimental groups of mice which were, WT, NLRP3$^{-/-}$, APP/PS1, and APP/PS1/NLRP3$^{-/-}$. Three-month-old animals were fed either a zinc normal or zinc deficient diet for six months before memory assessment using the Y-maze. As above, there was no effect of a zinc deficient diet on the memory of WT mice ($t(72)=-0.33$, $p=1.000$), or in NLRP3$^{-/-}$mice ($t(72)=-0.81$, $p=1.000$), (Fig. 5*A*). Also, as previously, the zinc deficient diet caused memory impairment in APP/PS1 mice ($t(72)=-8.06$, $p<0.001$), (Fig. 5*A*). However, the zinc deficiency-induced memory impairment in APP/PS1 mice was abolished in APP/PS1/NLRP3$^{-/-}$ mice ($t(72)=4.54$ $p<0.001$), (Fig. 5*A*). These data suggest that the effects of zinc deficiency on memory depend on NLRP3. These protective effects of NLRP3 deficiency on memory after zinc deficiency were independent of plaque burden or microglia activation as there was no significant difference in these parameters in APP/PS1 mice with or without NLRP3 (3-way interaction term: plaque $F(1,46)=1.15$, $p=0.290$; microglia $F(1,46)=0.49$, $p=0.488$), (Fig. 5*B-D*).

Discussion

Using patient data, animal models, and cell culture methods, we have provided evidence that zinc status is important in Alzheimer's disease progression, and specifically that zinc deficiency accelerated cognitive decline in an Alzheimer's disease model through potentiating inflammatory responses mediated by the NLRP3 inflammasome.

Our epidemiological evidence is supported by numerous previous studies which report that people with Alzheimer's disease have lower zinc serum levels (Ventriglia et al., 2015). Ventriglia *et al.* (2015) performed a meta-analysis resulting in a pooled sample of 1,064 people with Alzheimer's disease and 1,894 healthy controls and found that the serum or plasma zinc levels were lower in people with Alzheimer's disease with a standard mean difference of -0.39, providing initial evidence of a cause association of zinc deficiency and Alzheimer's disease. The present study takes this result further, demonstrating reduced cognitive decline over time in people with MCI and Alzheimer's disease in individuals who are taking zinc supplements. While we acknowledge that this association could be explained by an unaccounted hidden variable including life-style factors or unknown disease modifying medicines, most other mineral supplements were not associated with an improvement in cognitive decline. To probe this association and establish if zinc status had a causal effect on cognitive decline, we conducted *in vivo* experiments using animal models of amyloidopathy.

There is clinical and preclinical evidence that excessive zinc supplementation can lead to health complications by being directly toxic, inhibiting copper absorption and through an interaction with amyloidopathy mechanisms (Fosmire, 1990; Yang et al.,

724 2013; Flinn et al., 2014; Craven et al., 2018). There is also robust evidence for high
725 zinc deficiency prevalence among the elderly and in particular people with
726 Alzheimer's disease, hence, we hypothesise that the association of zinc
727 supplementation with improved cognitive outcomes reported here was likely due to
728 the mitigation of zinc deficiency, rather than zinc supplementation exceeding
729 recommended daily intake values (Briefel et al., 2000; Ventriglia et al., 2015).
730 Therefore, we designed the *in vivo* experiments to investigate the effects of mild sub-
731 clinical zinc deficiency on cognitive decline in the APP/PS1 mouse model of
732 Alzheimer's disease and addressed whether any effects could be reversed by
733 normalising the levels of zinc. From this we found that zinc deficient APP/PS1 mice
734 had accelerated cognitive decline, but these deficits could largely be reversed by
735 returning the mice to a diet which contained the recommended daily intake of zinc.
736
737 The literature describing the effects of zinc on amyloid deposition is complex (Esler
738 et al., 1996; Brown et al., 1997; Garai et al., 2007; Rezaei-Ghaleh et al., 2011;
739 Abelein et al., 2015; Lee et al., 2018). We report no changes in plaque deposition
740 induced through zinc deficiency and, therefore, we hypothesised zinc was
741 modulating the response to the Alzheimer's amyloidopathy modelled by the
742 APP/PS1 mice and not the amyloidopathy itself. Using the same animal model,
743 Stoltenberg *et al*. (2007) reported a mild increase in plaque size in zinc deficient
744 animals. However, the zinc deficiency induced by Stoltenberg *et al.* was more
745 severe, resulting in a 20% reduction in serum zinc levels. The present study induced
746 a mild subclinical zinc deficiency, which caused no change to serum zinc levels and
747 was only detected through reduced zinc levels in the bone. Brain levels of zinc were
748 not measured here due to the complication of amyloid plaques sequestering zinc.

749 Indeed Stoltenberg *et al.* could not detect changes in cortical zinc even with the more
750 severe zinc deficiency likely due to this sequestration effect.
751
752 We saw an increase in NLRP3 expression in the periplaque region in the
753 hippocampus of the APP/PS1 mice. This observation and previous research
754 supports an importance of NLRP3 in the response to amyloidopathy (Heneka et al.,
755 2013; Daniels et al., 2016). Using cellular models, we demonstrated that zinc
756 deficiency potentiated NLRP3 responses to stimuli including amyloid oligomers and
757 that zinc inhibited NLRP3 responses to activators such as silica. The concentration
758 of amyloid used was supraphysiological in order to observe measurable
759 inflammatory responses in the short time periods possible with the culture methods
760 utilised. This limitation was addressed by translating these results *in vivo*. We
761 established NLRP3 as the critical mechanism by which zinc deficiency accelerated
762 cognitive decline in the APP/PS1 mouse model through crossing NLRP3$^{-/-}$ and
763 APP/PS1 mouse lines. We demonstrated that the cognitive decline induced by zinc
764 deficiency was completely abated in the APP/PS1 mice deficient in NLRP3.
765 Interestingly, we saw no changes in amyloid deposition in the APP/PS1/ NLRP3$^{-/-}$
766 mice. Heneka *et* al. (Heneka et al., 2013) generated the same mouse strain and did
767 show reduced plaque burden, however, in that study 16-month-old mice were used.
768 Therefore, it may be the later stages of the pathology in which NLRP3 plays a role in
769 plaque deposition. Given the excellent research linking NLRP3 to the ageing process
770 (Youm et al., 2013), the age difference between Heneka et al. (Heneka et al., 2013)
771 and the present study could explain this difference.
772
773 Previous research has demonstrated that zinc chelation with clioquinol impedes the
774 MMP9 processing of pro-BDNF, perturbing synapse formation and cognitive

775 performance (Frazzini et al., 2018). Furthermore, zinc supplementation in the 3xTg
776 mouse model of Alzheimer's disease was found to prevent cognitive decline through
777 increasing BDNF levels and mitigating tau, amyloid and mitochondrial Alzheimer's
778 associated pathology (Corona et al., 2010). The RNAseq performed here found no
779 effects of zinc deficiency on expression of genes downstream of BDNF signalling
780 (e.g. neuropeptide Y). One explanation for this incongruence is the time frame and
781 severity of zinc deficiency. Zinc chelation likely induced a more severe reduction in
782 bioavailable zinc than what was observed in the present study. Additionally, Corona
783 *et al. (2010)* administered zinc supplementation to mice for 11 months, starting at 1-
784 month old mice. This was both a longer period than the present study and, began at
785 an age where neurodevelopment is ongoing. So, while in the present study we see
786 no evidence of BDNF modulation, it is likely this pathway is affected in other
787 modalities of zinc deficiency and supplementation.
788
789 Managing Alzheimer's disease is currently one of the greatest societal problems. An
790 increasing prevalence linked to an ageing population, with limited treatment options,
791 is creating a global crisis. The NLRP3 inflammasome has been identified as a
792 therapeutic target for the treatment of Alzheimer's disease and there are many
793 pharmaceutical and academic initiatives underway to develop new small molecule
794 inhibitors of the NLRP3 inflammasome (e.g. MCC950 and NBCs (Coll et al., 2015;
795 Baldwin et al., 2017)). The possibility of drug repurposing has also been identified for
796 targeting NLRP3 in Alzheimer's disease (Daniels et al., 2016). Here, we show that
797 coupled to these initiatives, the nutritional status, particularly of zinc, could be
798 assessed and used to treat groups of people with Alzheimer's disease shown to be
799 at risk of zinc deficiency. In theory zinc supplementation or dietary improvements
800 could be a cheap, rapid, low risk and easy enhancement to patient care.

Author Contributions

J Rivers-Auty: Data curation, formal analysis, investigation, methodology, project administration, and writing-original draft and review and editing.

VS Tapia: Investigation

CS White: Investigation

MJD Daniels: Investigation

S Drinkall: Investigation

PT Kennedy: Investigation

HG Spence: Investigation

S Yu: Investigation

JP Green: Investigation

C Hoyle: Investigation

J Cook: Investigation

A Bradley: Investigation

AE Mather: Data curation and formal analysis

R Peters: Data curation and formal analysis

T Tzeng: Generating and providing ASC-citrine mice and advising on their establishment and use.

MJ Gordon: Investigation

JH Beattie: Funding acquisition, conceptualization and methodology

D Brough: Conceptualization, funding acquisition, methodology, project administration, resources, supervision, and writing-original draft and review and editing.

CB. Lawrence: Conceptualization, funding acquisition, methodology, project administration, resources, supervision, and writing-original draft and review and editing.

References

Abelein A, Graslund A, Danielsson J (2015) Zinc as chaperone-mimicking agent for retardation of amyloid beta peptide fibril formation. Proc Natl Acad Sci U S A 112:5407-5412.

Alzheimers A Alzheimer's Association Report (2015) Alzheimer's disease facts and figures. Alzheimers & Dementia 11:332-384.

Baldwin AG, Rivers-Auty J, Daniels MJD, White CS, Schwalbe CH, Schilling T, Hammadi H, Jaiyong P, Spencer NG, England H, Luheshi NM, Kadirvel M, Lawrence CB, Rothwell NJ, Harte MK, Bryce RA, Allan SM, Eder C, Freeman S, Brough D (2017) Boron-Based Inhibitors of the NLRP3 Inflammasome. Cell Chem Biol 24:1321-1335 e1325.

Bates D, Machler M, Bolker BM, Walker SC (2015) Fitting Linear Mixed-Effects Models Using lme4. Journal of Statistical Software 67:1-48.

Beattie JH, Gordon MJ, Duthie SJ, McNeil CJ, Horgan GW, Nixon GF, Feldmann J, Kwun IS (2012) Suboptimal dietary zinc intake promotes vascular inflammation and atherogenesis in a mouse model of atherosclerosis. Mol Nutr Food Res 56:1097-1105.

Briefel RR, Bialostosky K, Kennedy-Stephenson J, McDowell MA, Ervin RB, Wright JD (2000) Zinc Intake of the U.S. Population: Findings from the Third National Health and Nutrition Examination Survey, 1988–1994. The Journal of Nutrition 130:1367S-1373S.

850 Brough D, Pelegrin P, Nickel W (2017) An emerging case for membrane pore
851 formation as a common mechanism for the unconventional secretion of FGF2
852 and IL-1β. J Cell Sci 130:3197-3202.
853 Brown AM, Tummolo DM, Rhodes KJ, Hofmann JR, Jacobsen JS, Sonnenberg-
854 Reines J (1997) Selective aggregation of endogenous beta-amyloid peptide
855 and soluble amyloid precursor protein in cerebrospinal fluid by zinc. J
856 Neurochem 69:1204-1212.
857 Browne J, Edwards DA, Rhodes KM, Brimicombe DJ, Payne RA (2017) Association
858 of comorbidity and health service usage among patients with dementia in the
859 UK: a population-based study. BMJ Open, p e012546.
860 Coll RC et al. (2015) A small-molecule inhibitor of the NLRP3 inflammasome for the
861 treatment of inflammatory diseases. Nat Med 21:248-255.
862 Corona C, Masciopinto F, Silvestri E, Viscovo AD, Lattanzio R, Sorda RL, Ciavardelli
863 D, Goglia F, Piantelli M, Canzoniero LM, Sensi SL (2010) Dietary zinc
864 supplementation of 3xTg-AD mice increases BDNF levels and prevents
865 cognitive deficits as well as mitochondrial dysfunction. Cell Death Dis 1:e91.
866 Craven KM, Kochen WR, Hernandez CM, Flinn JM (2018) Zinc Exacerbates Tau
867 Pathology in a Tau Mouse Model. J Alzheimers Dis 64:617-630.
868 Daniels MJ et al. (2016) Fenamate NSAIDs inhibit the NLRP3 inflammasome and
869 protect against Alzheimer's disease in rodent models. Nat Commun 7:12504.
870 Dempsey C, Rubio Araiz A, Bryson KJ, Finucane O, Larkin C, Mills EL, Robertson
871 AAB, Cooper MA, O'Neill LAJ, Lynch MA (2017) Inhibiting the NLRP3
872 inflammasome with MCC950 promotes non-phlogistic clearance of amyloid-
873 beta and cognitive function in APP/PS1 mice. Brain Behav Immun 61:306-
874 316.

875 Esler WP, Stimson ER, Jennings JM, Ghilardi JR, Mantyh PW, Maggio JE (1996)
876 Zinc-induced aggregation of human and rat beta-amyloid peptides in vitro. J
877 Neurochem 66:723-732.
878 Faux NG, Ritchie CW, Gunn A, Rembach A, Tsatsanis A, Bedo J, Harrison J,
879 Lannfelt L, Blennow K, Zetterberg H, Ingelsson M, Masters CL, Tanzi RE,
880 Cummings JL, Herd CM, Bush AI (2010) PBT2 rapidly improves cognition in
881 Alzheimer's Disease: additional phase II analyses. J Alzheimers Dis 20:509-
882 516.
883 Flinn JM, Bozzelli PL, Adlard PA, Railey AM (2014) Spatial memory deficits in a
884 mouse model of late-onset Alzheimer's disease are caused by zinc
885 supplementation and correlate with amyloid-beta levels. Front Aging Neurosci
886 6:174.
887 Fosmire GJ (1990) Zinc toxicity. The American Journal of Clinical Nutrition 51:225-
888 227.
889 Fournier DA, Skaug HJ, Ancheta J, Ianelli J, Magnusson A, Maunder M, Nielsen A, J
890 S (2012) AD Model Builder: usingautomatic differentiation for statistical
891 inference of highly parameterized complex nonlinear models. Optim Methods
892 Softw 27:233-249.
893 Frazzini V, Granzotto A, Bomba M, Massetti N, Castelli V, d'Aurora M, Punzi M, Iorio
894 M, Mosca A, Delli Pizzi S, Gatta V, Cimini A, Sensi SL (2018) The
895 pharmacological perturbation of brain zinc impairs BDNF-related signaling
896 and the cognitive performances of young mice. Sci Rep 8:9768.
897 Garai K, Sahoo B, Kaushalya SK, Desai R, Maiti S (2007) Zinc lowers amyloid-beta
898 toxicity by selectively precipitating aggregation intermediates. Biochemistry
899 46:10655-10663.

900 Gough M, Parr-Sturgess C, Parkin E (2011) Zinc metalloproteinases and amyloid
901 Beta-Peptide metabolism: the positive side of proteolysis in Alzheimer's
902 disease. Biochem Res Int 2011:721463.
903 Heneka MT, McManus RM, Latz E (2018) Inflammasome signalling in brain function
904 and neurodegenerative disease. Nat Rev Neurosci 19:610-621.
905 Heneka MT, Kummer MP, Stutz A, Delekate A, Schwartz S, Vieira-Saecker A, Griep
906 A, Axt D, Remus A, Tzeng TC, Gelpi E, Halle A, Korte M, Latz E, Golenbock
907 DT (2013) NLRP3 is activated in Alzheimer's disease and contributes to
908 pathology in APP/PS1 mice. Nature 493:674-678.
909 Hoyle C, Redondo-Castro E, Cook J, Tzeng TC, Allan SM, Brough D, Lemarchand E
910 (2020) Hallmarks of NLRP3 inflammasome activation are observed in
911 organotypic hippocampal slice culture. Immunology 161:39-52.
912 Hoyle C, Rivers-Auty J, Lemarchand E, Vranic S, Wang E, Buggio M, Rothwell NJ,
913 Allan SM, Kostarelos K, Brough D (2018) Small, Thin Graphene Oxide Is Anti-
914 inflammatory Activating Nuclear Factor Erythroid 2-Related Factor 2 via
915 Metabolic Reprogramming. ACS Nano 12:11949-11962.
916 Kambe T, Tsuji T, Hashimoto A, Itsumura N (2015) The Physiological, Biochemical,
917 and Molecular Roles of Zinc Transporters in Zinc Homeostasis and
918 Metabolism. Physiol Rev 95:749-784.
919 Lee MC, Yu WC, Shih YH, Chen CY, Guo ZH, Huang SJ, Chan JCC, Chen YR
920 (2018) Zinc ion rapidly induces toxic, off-pathway amyloid-beta oligomers
921 distinct from amyloid-beta derived diffusible ligands in Alzheimer's disease.
922 Sci Rep 8:4772.
923 Lenth RV (2016) Least-Squares Means: The R Package lsmeans. Journal of
924 Statistical Software 69:1-33.

925 Mariathasan S, Weiss DS, Newton K, McBride J, O'Rourke K, Roose-Girma M, Lee
926 WP, Weinrauch Y, Monack DM, Dixit VM (2006) Cryopyrin activates the
927 inflammasome in response to toxins and ATP. Nature 440:228-232.
928 Prasad AS (2012) Discovery of human zinc deficiency: 50 years later. J Trace Elem
929 Med Biol 26:66-69.
930 Profenno LA, Porsteinsson AP, Faraone SV (2010) Meta-Analysis of Alzheimer's
931 Disease Risk with Obesity, Diabetes, and Related Disorders. Biological
932 Psychiatry 67:505-512.
933 R Core Team (2018). R: A language and environment for statistical computing. R
934 Foundation for Statistical Computing, Vienna, Austria.
935 Rezaei-Ghaleh N, Giller K, Becker S, Zweckstetter M (2011) Effect of zinc binding on
936 beta-amyloid structure and dynamics: implications for Abeta aggregation.
937 Biophys J 101:1202-1211.
938 Rivers-Auty J, Mather AE, Peters R, Lawrence CB, Brough D (2020) Anti-
939 inflammatories in Alzheimer's disease-potential therapy or spurious correlate?
940 Brain Commun 2:fcaa109.
941 RStudio Team (2016) RStudio: Integrated Development for R. RStudio, Inc., Boston,
942 MA.
943 Sensi SL, Paoletti P, Bush AI, Sekler I (2009) Zinc in the physiology and pathology of
944 the CNS. Nat Rev Neurosci 10:780-791.
945 Skaug H, Fournier D, Nielsen A, Magnusson A, Bolker B (2013) Generalized Linear
946 Mixed Models using AD Model Builder. R package version 075.
947 Stoltenberg M, Bush AI, Bach G, Smidt K, Larsen A, Rungby J, Lund S, Doering P,
948 Danscher G (2007) Amyloid plaques arise from zinc-enriched cortical layers in
949 APP/PS1 transgenic mice and are paradoxically enlarged with dietary zinc
950 deficiency. Neuroscience 150:357-369.

951 Summersgill H, England H, Lopez-Castejon G, Lawrence CB, Luheshi NM, Pahle J,
952 Mendes P, Brough D (2014) Zinc depletion regulates the processing and
953 secretion of IL-1beta. Cell Death Dis 5:e1040.
954 Tzeng T-C, Schattgen S, Monks B, Wang D, Cerny A, Latz E, Fitzgerald K,
955 Golenbock DT (2016) A Fluorescent Reporter Mouse for Inflammasome
956 Assembly Demonstrates an Important Role for Cell-Bound and Free ASC
957 Specks during In Vivo Infection. Cell Reports 16:571-582.
958 Venegas C, Kumar S, Franklin BS, Dierkes T, Brinkschulte R, Tejera D, Vieira-
959 Saecker A, Schwartz S, Santarelli F, Kummer MP, Griep A, Gelpi E, Beilharz
960 M, Riedel D, Golenbock DT, Geyer M, Walter J, Latz E, Heneka MT (2017)
961 Microglia-derived ASC specks cross-seed amyloid-beta in Alzheimer's
962 disease. Nature 552:355-361.
963 Ventriglia M, Brewer GJ, Simonelli I, Mariani S, Siotto M, Bucossi S, Squitti R (2015)
964 Zinc in Alzheimer's Disease: A Meta-Analysis of Serum, Plasma, and
965 Cerebrospinal Fluid Studies. J Alzheimers Dis 46:75-87.
966 Webster SJ, Bachstetter AD, Nelson PT, Schmitt FA, Van Eldik LJ (2014) Using
967 mice to model Alzheimer's dementia: an overview of the clinical disease and
968 the preclinical behavioral changes in 10 mouse models. Front Genet 5:88.
969 White CS, Lawrence CB, Brough D, Rivers-Auty J (2017) Inflammasomes as
970 therapeutic targets for Alzheimer's disease. Brain Pathol 27:223-234.
971 Whitmer RA, Gunderson EP, Barrett-Connor E, Quesenberry CP, Yaffe K (2005)
972 Obesity in middle age and future risk of dementia: a 27 year longitudinal
973 population based study. British Medical Journal 330:1360-1362B.
974 Yang J, Harte-Hargrove LC, Siao CJ, Marinic T, Clarke R, Ma Q, Jing D, Lafrancois
975 JJ, Bath KG, Mark W, Ballon D, Lee FS, Scharfman HE, Hempstead BL

(2014) proBDNF negatively regulates neuronal remodeling, synaptic transmission, and synaptic plasticity in hippocampus. Cell Rep 7:796-806.

Yang Y, Jing X-P, Zhang S-P, Gu R-X, Tang F-X, Wang X-L, Xiong Y, Qiu M, Sun X-Y, Ke D, Wang J-Z, Liu R (2013) High dose zinc supplementation induces hippocampal zinc deficiency and memory impairment with inhibition of BDNF signaling. PLoS One 8:e55384-e55384.

Youm YH, Grant RW, McCabe LR, Albarado DC, Nguyen KY, Ravussin A, Pistell P, Newman S, Carter R, Laque A, Munzberg H, Rosen CJ, Ingram DK, Salbaum JM, Dixit VD (2013) Canonical Nlrp3 inflammasome links systemic low-grade inflammation to functional decline in aging. Cell Metab 18:519-532.

Figure legends

Figure 1: Zinc supplementation use was associated with reduced prevalence of Alzheimer's disease and slowed cognitive decline during disease development. ***A***) Table of baseline statistics by supplement showing nominal differences in nuisance variables such as age, gender, APOE4 status, and significant differences in the prevalence of cognitive dysfunction. Shown are the number of participants for each variable with percentage of total in brackets, or for numerical variables the means and standard deviations (SD) are shown. *$p < 0.05$, **$p < 0.01$, ***$p < 0.001$ compared to no supplement use. 'Statistics' column reports the omnibus tests. ***B***) A stacked bar chart showing the proportions of cognitive diagnosis. Zinc supplement use was associated with the lowest proportion of Alzheimer's disease. This was significantly different to 'no supplement' use group as reported in (***A***). Dashed lines represent proportions of cognitive diagnoses in the 'no supplement' group. ***C***) Summary table of the final negative binomial generalised linear mixed modelling (GLMM) with mini-mental state examination (MMSE) failures as the dependent variable. Zinc supplement use was associated with significantly slowed cognitive decline. Shown are the maximum likelihood estimates ("Estimate" columns) with Laplace estimates of the standard error ("Standard error" columns), Z-value and p-value from the Wald approximation ("p-value" columns), as well as, the significance of inclusion of the variable in the model evaluated using the log-likelihood ratio test - chi squared ("Statistics of inclusion" columns). ***D***) and ***E***) The effect of supplement use on predicted cognitive decline of a LMCI, 70-year-old female as measured by MMSE scores. Plots model the effect of zinc only supplement use (***E***) and any supplement (combined) use (***D***) with no supplement use modelled as the control group in both plots. CN = cognitively normal, EMCI and

1014 LMCI = early and late mild cognitive impairment, AD = Alzheimer's disease, ADAS =
1015 Alzheimer's disease assessment scale, MMSE = mini-mental state examination.

Figure 2: Subclinical zinc deficiency accelerates memory deficits in an animal model of Alzheimer's disease without effecting plasma zinc or weight gain. ***A***) Timeline of the zinc deficiency experiment in APPswe/PSδE9 (APP/PS1) and wild-type (WT) mice. ***B, C***) ICP-Mass spectrometry revealed that six months on a zinc deficient diet (ZD) (3 mg/kg) induced sustained subclinical zinc deficiency as measured by reduced bone zinc levels (***B***) but not plasma zinc levels (***C***). ***D***) ZD diet did not affect growth of the animals with no effect on body weight change during the course of the study. ***E, F***) The Y-maze memory task revealed that a ZD diet induced a significant memory deficit in the APP/PS1 mice compared to mice on a zinc normal diet (ZN, 35 mg/kg). These deficits were reversed by returning these mice onto a ZN for three months (ZD/ZN group; ***F***). ***G, H***) The novel smell recognition (NSR) task revealed significant deficits in the APP/PS1 ZD group compared to the ZN group (***H***). Animals returned to the ZN diet at six months old did not return to cognitive normal performance. In WT mice, no deficits were observed in the Y-maze or the NSR tasks on any diet combination (***E, G***). * $p < 0.05$, ***$p < 0.001$ compared to the ZN group within the same genotype. Holm-Sidak corrected post-hoc analysis. Data are presented as mean ± SEM. WT ZN, $n = 13$; WT ZD, $n = 15$; WT ZD/ZN, $n = 12$; APP/PS1 ZN, $n = 13$; APP/PS1 ZD, $n = 11$; APP/PS1 ZD/ZN, $n = 11$.

Figure 3: The effects of zinc deficiency alters the local response to the plaque without altering plaque burden or age-related cognitive decline. ***A***) Six months on a zinc deficient (ZD, 3 mg/kg) diet did not alter amyloidβ (Aβ) plaque burden in APPswe/PSδE9 (APP/PS1) mice compared to zinc normal (ZN, 35 mg/kg) controls.

The zinc recovery group was also unchanged (ZD diet for 3 months followed by a ZN diet for three months; ZD/ZN). ***B)*** Example images of Aβ plaque burden. ***C***) No differences were observed in microglia morphology between any diet combination, measured as percentage of microglia in an amoeboid phenotype. For ***A-C*** Sections were incubated with 6e10 (Aβ) or Iba1 (microglia) antibodies, visualised with DAB nickel (3,3'-diaminobenzidine, nickel sulphate) staining averaged across 6 coronal hippocampal sections per mouse, scale bars are 500μm. ***$p < 0.001$ main effect of genotype (2-way ANOVA). ***D,E***) Unlike in the APP/PS1 mouse, zinc deficiency did not accelerate age-related cognitive decline, as measured by the Y-maze, in 20-month-old C57B/6J mice placed on a ZD diet for three months. Similarly, no changes where observed in the 3-month-old 'young' C57B/6J controls. This suggested zinc deficiency was altering an amyloid specific response such as NLRP3-dependent inflammation.

(***F, G***) Zinc content in the diet had no effect on the transcriptome in whole hippocampal tissue of APP/PS1 and wild-type (WT) mice. ***F***) a principal component analysis (PCA) of the transcriptome data showing no clustering of the WT or APP/PS1 mice or the ZD and ZN diet. ***G***) Volcano plot of genes comparing APP/PS1 mice on a ZN or ZD diet showing minimal effects of diet with only one gene found to be significantly different following false discovery rate (FDR) adjustment (n = 6/group). ***H & I***) To establish if there was a local response in APP/PS1 mice, peri-plaque regions (100 μm diameter) and plaque free tissue from 8-9-month-old APP/PS1 mice were isolated using laser capture (***H***) and probed for the plaque-associated gene TREM2 (***I i***) and the inflammatory genes NLRP3 (***I ii***) and IL-1β (***I iii***), and from this it was found that the NLRP3/IL-1β response is very tightly associated to the peri-plaque region (n = 3, for all groups). **$p < 0.01$ and ***$p < 0.001$ versus plaque containing region. Plaques were identified with Congo red

staining. Holm-Sidak corrected post-hoc analysis. Data are presented as mean ± SEM. For ***A-C***, WT ZN, *n* = 13; WT ZD, *n* = 15; WT ZD/ZN, *n* = 12; APP/PS1 ZN, *n* = 13; APP/PS1 ZD, *n* = 11; APP/PS1 ZD/ZN, *n* = 11. For ***D,E,*** Young ZN, *n* =15, Young ZD, *n* = 15, Aged ZN, *n* = 11, Aged ZD, *n* = 12 (<15 due to attrition

Figure 4: Zinc deficiency activates the NLRP3 inflammasome and potentiates NLRP3 responses to stimuli, while zinc supplementation inhibits NLRP3 activation. *A-D*) Primary bone marrow derived macrophages (BMDMs) experiments demonstrating zinc deficiency activates the NLRP3 inflammasome and zinc supplementation inhibits NLRP3 inflammasome activation. **A**) Enhanced IL-1β release from zinc deficient macrophages (BMDM) which were primed with lipopolysaccharide (LPS, 1 μg/ml, 4 h) and then treated with increasing concentrations of the zinc chelation agent TPEN for 4 h. ***B***) BMDMs were primed (LPS 1 μg/ml, 4 h) and treated with TPEN (10 μM) with and without NLRP3 inhibition by MCC950 (10 μM) (**i**) or silica (300μg/ml) with and without $ZnCl_2$ (200 μM) supplementation (**ii**); the cells were lysed in the media and probed for ASC oligomerisation, IL-1β cleavage (17kd), caspase 1 activation (p10) and gasdermin D cleavage. ***C***) Zinc supplementation inhibits IL-1β release; BMDMs were primed (LPS 1 μg/ml, 4 h) and treated with silica (300 μg/ml) in the presence of increasing concentrations of $ZnCl_2$. ***D***) BMDMs treated with TPEN (10 μM) and amyloid oligomers (10 μg/ml, N.B no LPS priming) for 24 h release IL-1β which is inhibited by MCC950 treatment (10 μM). **p* < 0.05, ***p* < 0.01 and ****p* < 0.001 versus no treatment or LPS control. ###*p* < 0.001 versus activated group (Amyloid+TPEN). ***E &*** ***F***) Confirmation experiments in mixed glial cultures demonstrating that LPS-primed BMDMs and mixed glial cultures have similar NLRP3 responses to zinc deficiency. ***E***) Zinc deficient primary mixed glia release IL-1β in an NLRP3 dependent manner;

primary murine mixed glia were primed with LPS (1 μg/ml, 4 h) and then treated with TPEN (10 μM) or silica (300 μg/ml) for 4 h with and without the NLRP3 inhibitor MCC950 (10 μM). ***F***) LPS (1 μg/ml, 4 h) primed mixed glia release more IL-1β in response to amyloid oligomers (10 μg/ml, 4 h) when zinc deficiency is induced (TPEN, 10 μM). ***p* < 0.01 versus LPS alone control. #*p* < 0.05 versus activated group (LPS/silica or LPS/TPEN). ***G & H***) Zinc deficient (TPEN 10 μM) primary ASC-citrine expressing microglia (primed with LPS; 1 μg/ml, 2 h) form inflammasome specks over time (***G,Hii,*** white arrows) which is inhibited by the NLRP3 inhibitors MCC950 (10 μM)(***Hiii***) and NBC19 (2 μM) (***Hiv***). ****p* < 0.001 versus vehicle control (LPS alone). ###*p* < 0.001 versus activated group (LPS/TPEN). Holm-Sidak corrected post-hoc analysis following one-way (***A,C,D***), two-way (***E,F***) or repeated measures (***G***) ANOVA. Data are presented as mean ± SEM of 4 independent experiments.

Figure 5: Zinc deficiency accelerates cognitive decline in the APP/PS1 mouse model of Alzheimer's disease through an NLRP3 dependent mechanism. ***A***) APP/PS1 and C57BL/6J (wild-type; WT) littermate mice were crossed with NLRP3$^{-/-}$ mice. Three-month-old mice from each genotype combination were placed on a zinc deficient (ZD, 3 mg/kg) or zinc normal (ZN, 35 mg/kg) diet for six months and were then assessed using the Y-maze memory task. Memory deficits were seen in the APP/PS1 mice on a ZD diet but not on a ZN diet. However, APP/PS1/ NLRP3$^{-/-}$ mice on a ZD diet did not have memory deficits. ***B,D***) No effect of diet or genotype was seen on Aβ plaque burden in APP/PS1 mice, or on ***C***) microglia morphology measured as percentage of microglia in an amoeboid phenotype in adjacent sections. For ***B*** and ***C*** sections were incubated with 6e10 (Aβ) and Iba1 (microglia) antibodies, respectively, visualised with DAB nickel (3,3'-diaminobenzidine, nickel

sulphate) staining averaged across 6 sagittal hippocampal sections per mouse, scale bars are 250μm. ***p <0.001 versus WT littermates of the same NLRP3 genotype and diet. ##p < 0.01 versus NLRP3$^{-/-}$ group of the same diet and APP/PS1 genotype conditions. Holm-Sidak corrected post-hoc analysis following three-way ANOVA (NLRP3 genotype, diet, APP/PS1 genotype). Data are presented as mean ± SEM. WT/NLRP3$^{+/+}$ ZN, n = 12; WT/NLRP3$^{+/+}$ ZD, n = 14; WT/NLRP3$^{-/-}$ ZN, n = 8; WT/NLRP3$^{-/-}$ ZD, n = 9; APP/PS1/NLRP3$^{+/+}$ ZN, n = 8; APP/PS1/NLRP3$^{+/+}$ ZD, n = 11; APP/PS1/NLRP3$^{-/-}$ ZN, n = 13; APP/PS1/NLRP3$^{-/-}$ ZD, n = 9.

Extended data. The extended data contains the annotated R code and output of the epidemiological analysis of the Alzheimer's disease neuroimaging cohort study.

1020

Table 1. Diet composition

Diet component	g/kg
Egg white solids	212
Maltodextrin	75
Sucrose	327
Corn Starch	186.5
Corn Oil	100
Cellulose	46.236
Mineral Mix (zinc absent)	35
Calcium phosphate, dibasic	3
Chromium Potassium Sulfate, dodecahydrate	0.01
Vitamin Mix AIN 93	10
Biotin	0.004
p-Aminobenzoic Acid	0.11
Vitamin C, ascorbic acid, coated (97.5%)	1.017
Choline Bitartarate	3
Inositol	0.11
Zinc chloride (3mg/kg) (Zinc deficient)	0.0052
Zinc chloride (35mg/kg) (Zinc normal)	0.0719

1021 The composition of the zinc normal (35 mg/kg) and zinc
1022 deficient (3 mg/kg) diets were identical apart from the
1023 amount of zinc.

A

	No supplement	Calcium	Iron	Magnesium	Multi-vitamin	Selenium	Zinc	Statistics
Diagnosis								
CN	131 (20%)	185 (31%)	35 (32%)	60 (37%)	161 (31%)	17 (40%)	20 (31%)	$X^2(18)=92.5$ p<0.0001
EMCI	129 (20%)	116 (20%)	29 (26%)	32 (20%)	70 (13%)	3 (7%)	15 (23%)	
LMCI	219 (33%)	199 (33%)	37 (33%)	54 (33%)	199 (31%)	18 (42%)	26 (40%)	
AD	176(26%)	89 (15%)***	10 (9%)**	16 (10%)***	94 (18%) ns	5 (12%) ns	4 (6%)**	
ADAS (mean, SD)	18.9 (10.1)	15.8 (9.1)***	14.8 (8.3) ns	14.1 (9.0)**	17.0 (9.3) ns	14.7 (7.0) ns	14.2 (6.9) ns	$X^2(6)=48.7$ p<0.0001
MMSE (mean, SD)	26.4 (2.8)	27.3 (2.6)***	27.2 (2.6) ns	28.0 (2.4)*	27.7 (2.2) ns	27.6 (2.4) ns	27.4 (2.5) ns	$X^2(6)=50.0$ p<0.0001
Gender								
Male	232 (35%)	385 (65%)	56 (50%)	91 (56%)	200 (38%)	14 (33%)	25 (38%)	$X^2(6)=143.0$ p<0.0001
Female	423 (65%)	204 (35%)	55 (50%)	71 (44%)	324 (62%)	29 (67%)	40 (62%)	
Age (mean, SD)	73.7 (7.5)	73.8 (7.0)**	74.3 (7.1) ns	72.9 (6.7)*	74.4 (7.1)*	74.5 (6.2) ns	73.4 (7.1) ns	$F(6)=1.46$ p=0.1874
APOE4								
-/-	315 (48%)	321 (54%)	68 (61%)	86 (53%)	292 (56%)	23 (55%)	37 (57%)	$X^2(12)=15.3$ p=0.223
+/-	261 (40%)	209 (35%)	32 (29%)	62 (38%)	185 (35%)	16 (36%)	25 (38%)	
+/+	79 (12%)	59 (10%)	11 (10%)	14 (9%)	47 (9%)	4 (9%)	3 (5%)	
Education								
Primary	223 (34%)	200 (34%)	37 (33%)	57 (35%)	193 (37%)	26 (60%)	22 (34%)	$X^2(18)=29.3$ p=0.045
Secondary	197 (37%)	155 (26%)	26 (23%)	48 (30%)	151 (29%)	10 (23%)	24 (37%)	
Tertiary	115 (15%)	136 (23%)	30 (27%)	30 (19%)	102 (20%)	4 (9%)	10 (15%)	
Post-graduate	120 (14%)	98 (17%)	18 (16%)	27 (17%)	78 (17%)	3 (7%)	9 (14%)	
Headache	42 (6%)	65 (11%)	10 (9%)	14 (8%)	48 (9%)	5 (11%)	4 (6%)	$X^2(6)=9.5$ p=0.1495
Arthritis	213 (33%)	261 (44%)	57 (51%)	70 (43%)	226 (43%)	19 (44%)	31 (48%)	$X^2(6)=29.8$ P<0.0001
Diabetes	42 (4%)	37 (4%)	14 (8%)	9 (4%)	47 (6%)	2 (3%)	7 (7%)	$X^2(6)=10.7$ p=0.0980
Smoker	176 (27%)	140 (24%)	30 (27%)	44 (27%)	129 (24%)	11 (24%)	11 (16%)	$X^2(6)=4.6$ p=0.600
Cardiovascular risk factors	413 (63%)	346 (59%)	70 (63%)	91 (56%)	322 (61%)	25 (58%)	40 (61%)	$X^2(6)=4.4$ p=0.6267
Total	**655**	**509**	**111**	**162**	**524**	**43**	**65**	

B

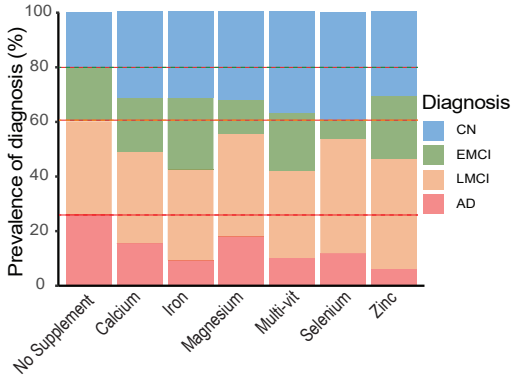

C

	Main Effect				Interaction Effect (with time)			
	Estimate	Standard Error	p-value	Statistics of inclusion	Estimate	Standard Error	p-value	Statistics of inclusion
Diagnosis								
CN	-	-	-		-	-	-	
EMCI	0.708	0.066	p<0.00001	$\chi^2(3)=1147$, p<0.00001	-0.00332	0.0010	p=0.00145	$\chi^2(3)=79.8$, p<0.00001
LMCI	1.242	0.056	p<0.00001		0.00286	0.0007	p=0.00008	
AD	2.11	0.062	p<0.00001		0.00880	0.0014	p<0.00001	
Age	0.018	0.003	p<0.00001	$\chi^2(1)=48.2$, p<0.00001	-	-	-	-
Gender								
Female	-	-	-	$\chi^2(1)=2.2$, p=0.138010	-	-	-	$\chi^2(2)=8.4$, p=0.003752
Male	0.096	0.040	p=0.01806		-0.00172	0.0006	p=0.00355	
APOE4								
-/-	-	-	-		-	-	-	
+/-	0.121	0.042	p=0.00446	$\chi^2(2)=60.6$, p<0.00001	0.00588	0.0006	p<0.00001	$\chi^2(2)=120.6$, p<0.00001
+/+	0.226	0.065	p=0.00048		0.00777	0.0009	p<0.00001	
Education								
Primary	0.352	0.057	p<0.00001	$\chi^2(3)=47.4$, p<0.00001	-0.00250	0.0008	p=0.00224	$\chi^2(3)=26.6$, p<0.00001
Secondary	0.362	0.056	p<0.00001		-0.00226	0.0008	p=0.00532	
Tertiary	0.2	0.050	p=0.00005		-0.00375	0.0007	p<0.00001	
Post-graduate	-	-	-		-	-	-	
Calcium	0.09880	0.04305	p=0.02172	$\chi^2(1)=3.0$, p=0.08326	0.00117	0.0006	p=0.05361	$\chi^2(1)=3.8$, p=0.05125
Iron	0.12126	0.0758	p=0.11007	$\chi^2(1)=0.8$, p=0.37110	0.00192	0.0008	p=0.02023	$\chi^2(1)=5.4$, p=0.02014
Magnesium	0.11233	0.06666	p=0.09198	$\chi^2(1)=4.4$, p=0.03594	0.00059	0.0009	p=0.49260	$\chi^2(1)=0.4$, p=0.5271
Multi-vitamin	0.00351	0.04150	p=0.93250	$\chi^2(1)=0$, p=0.99999	0.00024	0.0006	p=0.68480	$\chi^2(1)=0.2$, p=0.65470
Selenium	0.10269	0.12239	p=0.40145	$\chi^2(1)=2.2$, p=0.13800	0.00218	0.0014	p=0.11098	$\chi^2(1)=2.6$, p=0.10690
Zinc	0.07117	0.09972	p=0.04755	$\chi^2(1)=2.2$, p=0.13800	0.00207	0.0007	p=0.00511	$\chi^2(1)=7.4$, p=0.00540
All Supplements	0.03760	0.04024	p=0.35018	$\chi^2(1)=1.2$, p=0.27330	0.00023	0.0006	p=0.71872	$\chi^2(1)=0.2$, p=0.65470

D

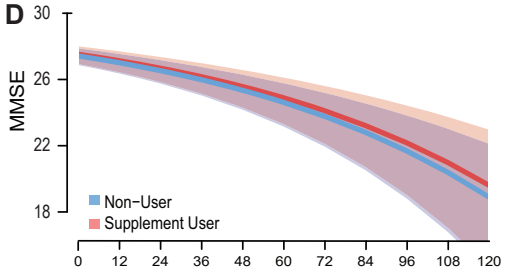

E